Discrete Cell Model of Fixed-Bed Adsorbers with Rectangular Adsorption Isotherms

Adsorption of organics into activated carbon particles within a fixed-bed adsorber is modeled using the concept of mixing cells. The adsorption isotherm of these organics is taken to be rectangular because of the commonly observed strong affinity of organics into activated carbons. The model equations are solved by a singular perturbation method, and this results in a graphical procedure similar to that of McCabe and Thiele used in distillation column design. Such a graphical procedure provides a quick means to determine the adsorbate profiles along the adsorber for a given time and also the breakthrough curve, which reflects the performance of the adsorber.

D. D. DO

Department of Chemical Engineering
University of Queensland
St. Lucia., Qld. 4067, Australia

SCOPE

Activated carbon is increasingly used in many fields of engineering. Its high internal surface area (of order of 1000 m^2/g) and high affinity to many organic solutes in aqueous phase have resulted in its wide use in water treatment. The adsorption isotherm of these organic solutes in activated carbon is usually very sharp at very low concentrations and is rather flat for concentrations away from the very low range. Such an isotherm is ideally approximated by a rectangular isotherm (i.e., irreversible isotherm). This is, in fact, practical because the practical range of concentrations is usually outside the very low concentration range. Because of the popular use of activated carbon and its interesting rectangular isotherm, this theoretical analysis will deal exclusively with such adsorbent in a fixed-bed adsorber. Simple graphical procedure results from the use of a discrete cell model for the adsorber, and an explicit design algorithm is presented.

CONCLUSIONS AND SIGNIFICANCE

A discrete cell model has been used in the theoretical analysis of a fixed-bed adsorber for systems having a rectangular adsorption isotherm. A powerful method of singular perturbation was applied during the course of analysis that has resulted in a graphical procedure to determine the solute and the adsorption profile along the adsorber. Most importantly, the analysis also yields a graphical procedure to determine a breakthrough curve that reflects the performance of the adsorber. It was found that the breakthrough curves exhibit a constant pattern shape for all values of fluid velocity. This constant pattern shape was found to vary very slightly with the degree of axial mixing. For practical design engineers, a simple explicit design algorithm is presented to design a fixed-bed adsorber and to determine its lifetime for given throughput and inlet adsorbate concentration.

INTRODUCTION

Adsorption process is increasingly gaining wide applications in many practical fields, for example, chemical engineering, biochemical engineering, food engineering, medical engineering, and wastewater treatment, to name a few. To successfully design such a process, one often uses a simple batch adsorber to extract equilibrium and dynamic parameters, i.e., the equilibrium isotherm and the effective diffusivity. The isotherm dictates the capacity of the solid, while the effective diffusivity controls the global rate of adsorption. Once these parameters are confidently extracted, one is then able to design a continuous process for adsorption. Very often, one is apt to choose a fixed-bed configuration for his design. Table 1 lists numerous researchers who have used this fixed-bed configuration in their adsorption studies.

Knowing the parameters from the batch studies, one must use a fixed-bed diffusion-adsorption model to predict the lifetime of the continuous adsorber. Many investigators (Rimpel et al., 1967; Colwell and Dranoff, 1969; Brauch and Schlünder, 1975; Carleton et al., 1978; Miura et al., 1979, 1983; Crittenden et al., 1980; Van Vliet et al., 1980; Weber and Liu, 1980; Santacesaria et al., 1982) have used the classical dispersion model to predict the lifetime, which is reflected in the breakthrough curve.

In the study of adsorption of organic solutes onto activated car-

TABLE 1. PAST ADSORPTION STUDIES IN FIXED BEDS

Authors	Solid	Model	Isotherm
Masamune and Smith (1964)	Vycorglass	Pore	Linear
Rimpel et al. (1967)	Alumina	Combined	Linear
Schneider and Smith (1968a)	Silica gel	Pore	Linear
Schneider and Smith (1968b)	Silica gel	Combined	Linear
Colwell and Dranoff (1969)	Ion exchange resin	Surface	Linear
Hashimoto and Smith (1973)	Zeolite 5A	Pore	Linear
Galan et al. (1975)	Activated carbon	Pore	Linear
Brauch and Schlünder (1975)	Activated carbon	Pore	Rectangular
Ozil and Bonnetain (1977)	Zeolite 13X	Surface	Linear
Shah and Ruthven (1977)	Zeolite 5A	Surface	Linear
Carleton et al. (1978)	Alumina	Pore	Linear
Miura et al. (1979)	Activated carbon	Pore	Langmuir
Crittenden et al. (1980)	Activated carbon	Surface	Langmuir
Van Vliet et al. (1980)	Activated carbon	Surface	Freundlich
Johansson and Neretnieks (1980)	Activated carbon	Pore, surface	Freundlich
Andrieu and Smith (1980)	Activated carbon	Pore	Linear
Seirafi and Smith (1980)	Activated carbon	Pore	Linear
Weber and Liu (1980)	Activated carbon	Surface	Freundlich
Lee et al. (1981)	Zeolite 3A, 5A, 13X	Pore	Linear
Santacesaria et al. (1982)	Zeolite Y	Pore	Langmuir
Kumar et al. (1982)	Zeolite 4A, 5A	Pore	Linear
Lee et al. (1982)	Zeolite 5A	Pore	Linear
Miura et al. (1983)	Activated carbon	Pore	Langmuir

bon, many researchers (Brauch and Schlünder, 1975; Suzuki and Kawazoe, 1974; Spahn and Schlünder, 1975) have found that the isotherm is rather flat, i.e., an irreversible isotherm or a rectangular isotherm. Such an isotherm is commonly observed in the adsorption of organic solutes onto activated carbon because of the strong affinity between the adsorbates and the adsorbent.

In this paper we shall employ a discrete cell model to analyze a fixed-bed adsorption system having a rectangular adsorption isotherm. The model equations will be solved by a singular perturbation method, and this results in a graphical procedure similar to that of McCabe and Thiele used in distillation column design. Such a graphical procedure provides a quick and simple means to determine the breakthrough curve and also the adsorbate profile along the adsorber. It is noted that a similar treatment of the concepts was presented by Cooper and Liberman (1970) and Neretnicks (1974) in their analysis of a fixed-bed adsorption under the conditions of pore diffusion control and irreversible isotherm. The exception is that this analysis includes axial dispersion. Also, a full analytical solution to a fixed-bed breakthrough curve that is simple enough to use with a desk calculator has no need for graphical procedures.

THEORY

Consider a fixed-bed adsorber containing porous solid adsorbents. The fixed-bed adsorber can be modeled as a series of mixing cells adsorbers. The number of mixing cells depends on the degree of axial dispersion in the fixed-bed adsorber. The number of mixing cells is

$$N = \frac{1}{2}\frac{UL}{E} \tag{1}$$

where U is the superficial velocity, L is the length of the adsorber, and E is the axial dispersion coefficient. Application of the mixing cell model to fixed-bed reactors has been carried out by Deans and Lapidus (1960) and Cho et al. (1983). The concept of the mixing cell model is now applied to a fixed-bed adsorber.

In this analysis, we assume that:

- Solid adsorbent particle is of spherical geometry.
- Adsorption is very strong compared to desorption and diffusion (i.e., $\phi \gg 1$).
- There is constant effective diffusivity.
- System is isothermal.

The material balance of the solute in the pore fluid of particles within the $(n+1)$th cell is:

$$\epsilon_p \frac{\partial C^{n+1}}{\partial t} = D_e \frac{1}{r^2}\frac{\partial}{\partial r}\left(r^2 \frac{\partial C^{n+1}}{\partial r}\right) - \rho_p k C^{n+1}\left(1 - \frac{q^{n+1}}{q_m}\right) \tag{2}$$

when C^{n+1} is the pore fluid concentration in the $(n+1)$th cell, ϵ_p is the particle voidage, D_e is the effective diffusivity, ρ_p is the particle density, q^{n+1} is the solute concentration on the adsorbed phase, q_m is its maximum concentration, and k is the adsorption rate constant.

The material balance of the solute on the adsorbed phase of the $(n+1)$th cell is

$$\frac{\partial q^{n+1}}{\partial t} = k C^{n+1}\left(1 - \frac{q^{n+1}}{q_m}\right) \tag{3}$$

The initial and boundary of Eqs. 2 and 3 are

$$t = 0; \quad C^{n+1} = q^{n+1} = 0 \tag{4}$$

$$r = 0; \quad \partial C^{n+1}/\partial r = 0 \tag{5a}$$

$$r = R; \quad D_e \frac{\partial C^{n+1}}{\partial r} = k_m (C_b^{n+1} - C^{n+1}) \tag{5b}$$

where

R = radius of the adsorbent

k_m = mass transfer coefficient

The solute mass balance in the $(n+1)$th mixing cell is

$$\epsilon V \frac{dC_b^{n+1}}{dt} = F(C_b^n - C_b^{n+1}) - \frac{3(1-\epsilon)}{R} D_e \left.\frac{\partial C^{n+1}}{\partial r}\right|_R \tag{6}$$

where ϵ is the bed voidage, V is the volume of one mixing cell (void and solid volume) ($V = V_T/N$; V_T is the total adsorber volume), F is the flow rate, and C_b^{n+1} is the solute concentration in the $(n+1)$th cell. The pertinent initial condition of Eq. 6 is

$$t = 0; \quad C_b^{n+1} = 0 \tag{7}$$

By defining the following nondimensional variables and parameters

$$A^{n+1} = C^{n+1}/C_{bo},\ A_s^{n+1} = q^{n+1}/q_m,\ A_b^{n+1} = C_b^{n+1}/C_{bo} \tag{8a}$$

$$x = r/R,\ \tau = D_e t/\epsilon_p R^2,\ \phi^2 = \rho_p k R^2/D_e \tag{8b}$$

$$\psi = \epsilon_p C_{bo}/\rho_p q_m,\ \alpha = \frac{\epsilon_p F R^2}{\epsilon V D_e},\ \beta = \frac{3\epsilon_p(1-\epsilon)}{\epsilon} \tag{8c}$$

$$Bi = k_m R/D_e \tag{8d}$$

Equations 2–7 become

$$\frac{\partial A^{n+1}}{\partial \tau} = \frac{1}{x^2}\frac{\partial}{\partial x}\left(x^2\frac{\partial A^{n+1}}{\partial x}\right) - \phi^2 A^{n+1}(1 - A_s^{n+1}) \tag{9a}$$

$$\frac{\partial A_s^{n+1}}{\partial \tau} = \psi\phi^2 A^{n+1}(1 - A_s^{n+1}) \tag{9b}$$

$$\frac{dA_b^{n+1}}{d\tau} = \alpha(A_b^n - A_b^{n+1}) - \beta\left.\frac{\partial A^{n+1}}{\partial x}\right|_1 \tag{9c}$$

$$\tau = 0; \quad A^{n+1} = A_s^{n+1} = A_b^{n+1} = 0 \tag{9d}$$

$$x = 0; \quad \partial A^{n+1}/\partial x = 0 \tag{9e}$$

$$x = 1; \quad \frac{1}{Bi}\cdot\frac{\partial A^{n+1}}{\partial x} = A_b^{n+1} - A^{n+1} \tag{9f}$$

for $n = 0,1,2,\ldots,N-1$. Here $A_b^0 = 1$.

Single Particle Analysis in the $(n+1)$th Mixing Cell

Before solving the full model equations describing the concentration changes in the particle and in the reservoir, it is more logical to consider the dynamic response of a single adsorbent particle exposed to an environment of concentration A_b^{n+1}.

Based on our assumption b in the previous section, the nondimensional parameter is a very large number ($\phi \gg 1$). In physical terms, this corresponds to the flat part of a Langmuir isotherm and a very fast adsorption rate compared to diffusion rate. Furthermore, the parameter ψ, which measures the amount in the pore fluid compared to the amount in the solid phase, is always very small for many practical adsorption systems ($\psi \ll 1$). Thus we have the following two small parameters at our disposal:

$$\frac{1}{\phi} \ll 1, \text{ and } \psi \ll 1 \tag{10}$$

Because of the large capacity of the solid adsorbents, the proper time scale to observe such uptake is

$$\tilde{t} = \psi\tau \tag{11}$$

In terms of this time scale, Eqs. 9a–c become

$$\psi\mu^2\frac{\partial A^{n+1}}{\partial \tilde{t}} = \mu^2\frac{1}{x^2}\frac{\partial}{\partial x}\left(x^2\frac{\partial A^{n+1}}{\partial x}\right) - A^{n+1}(1 - A_s^{n+1}) \tag{12a}$$

$$\mu^2\frac{\partial A_s^{n+1}}{\partial \tilde{t}} = A^{n+1}(1 - A_s^{n+1}) \tag{12b}$$

$$\psi\frac{dA_b^{n+1}}{d\tilde{t}} = \alpha(A_b^n - A_b^{n+1}) - \beta\left.\frac{\partial A^{n+1}}{\partial x}\right|_1 \tag{12c}$$

$$\text{where } \mu = \frac{1}{\phi} \ll 1. \tag{13}$$

Applying the matched asymptotic expansion procedure, described in Do (1982) in the context of noncatalytic gas solid reaction, we obtain

$$\frac{dX^{n+1}}{d\tilde{t}} = -\frac{A_b^{n+1}}{X^{n+1}\left[1 - \left(1 - \frac{1}{Bi}\right)X^{n+1}\right]} \tag{14}$$

and

$$\alpha(A_b^n - A_b^{n+1}) - \frac{\beta A_b^{n+1}}{\left[\frac{1}{X^{n+1}} - 1 + \frac{1}{Bi}\right]} = 0 \tag{15}$$

where X^{n+1} is the adsorption front of the $(n+1)$th cell. Thus the speed of the adsorption front with respect to the time scale $\tilde{t}$ is proportional to the solute concentration in the reservoir A_b^{n+1} and is a function of its own location and the degree of mixing Bi, as shown in the denominator of Eq. 14. The pertinent initial condition of Eq. 14 is

$$\tilde{t} = 0; \quad X^{n+1} = 1 \tag{16}$$

The integration of Eq. 14, subject to the initial condition, 16, is feasible only when A_b^{n+1} is a function of X^{n+1} or is a known function of time.

Mixing Cell Analysis

Equation 15 can be rewritten as

$$\frac{A_b^{n+1}}{A_b^n} = \frac{1}{1 + \frac{(\beta/\alpha)}{[1/X^{n+1} - 1 + 1/Bi]}} = G^{n+1} \tag{17}$$

The right-hand side of Eq. 29 is merely the transfer function of the $(n+1)$th cell, i.e., a concept introduced by Cho et al. (1983).

Thus the complete final equations for the $(n+1)$th mixing cell are Eqs. 14, 16, and 17. So if the solute concentration of the nth mixing cell A_b^n is a known function of time, Eq. 17 can be substituted into Eq. 14 and the resulting equation can be integrated to obtain the adsorption front of the $(n+1)$th mixing cell. The solute concentration in that cell is then given in Eq. 17. In short, such a procedure allows one to predict the adsorption front in the $(n+1)$th mixing cell from the known solutions of the nth mixing cell.

Substituting Eq. 17 into Eq. 14 and integrating with respect to $\tilde{t}$ gives

$$[1 - (X^{n+1})^2] + \frac{2}{3}\left(\frac{\beta}{\alpha} + \frac{1}{Bi} - 1\right) \times [1 - (X^{n+1})^3] = 2\int_0^t A_b^n(\tilde{t})d\tilde{t} \tag{18}$$

Thus the time required (T_{n+1}) for the adsorption front of the $(n+1)$th mixing cell to reach the particle center is

$$\frac{1}{3} + \frac{2}{3}\left(\frac{\beta}{\alpha} + \frac{1}{Bi}\right) = 2\int_0^{T_{n+1}} A_b^n(\tilde{t})d\tilde{t} \tag{19}$$

or

$$1 + 2\left(\frac{\beta}{\alpha}\right) + \frac{2}{Bi} = 6\int_0^{T_{n+1}} A_b^n(\tilde{t})d\tilde{t} \tag{20}$$

Breakthrough Curve and Adsorber Lifetime

The solute in each mixing cell is a function of time, and the transient response of solute of the last mixing cell (called the breakthrough curve) reflects the performance of the adsorber. First

consider the first mixing cell (setting n to 0 in Eqs. 17 and 18 and noting that $A_b^0 = 1$):

$$A_b^1 = \frac{1}{\left[1 + \dfrac{(\beta/\alpha)}{(1/X^1 - 1 + 1/Bi}\right]} \tag{21}$$

and

$$[1 - (X^1)^2] + \frac{2}{3}\left(\frac{\beta}{\alpha} + \frac{1}{Bi} - 1\right)[1 - (X^1)^3] = 2\tilde{t} \tag{22}$$

For the $(n + 1)$th mixing cell, we arrange Eq. 18 as follows:

$$[1 - (X^{n+1})^2] + \frac{2}{3}\left(\frac{\beta}{\alpha} + \frac{1}{Bi} - 1\right)[1 - (X^{n+1})^3] = 2\int A_b^n \cdot \frac{d\tilde{t}}{dX^n} \cdot dX^n \tag{23}$$

Combining Eqs. 14 and 23 yields

$$[1 - (X^{n+1})^2] + \frac{2}{3}\left(\frac{\beta}{\alpha} + \frac{1}{Bi} - 1\right)[1 - (X^{n+1})^3] = [1 - (X^n)^2] + \frac{2}{3}\left(\frac{1}{Bi} - 1\right)[1 - (X^n)^3] \tag{24}$$

Thus the adsorption front of the $(n + 1)$th mixing cell is directly related to that of the nth mixing cell. Therefore, knowing the adsorption front of the first mixing cell as given in Eq. 22, those of the second, third, and so on, mixing cells can be easily calculated from Eq. 24. The corresponding solute concentrations, then, can be calculated from Eq. 17.

The time required for the adsorption front to reach the particle center of the first mixing cell is (from Eq. 22)

$$T_1 = \frac{1}{6} + \frac{1}{3}\left(\frac{\beta}{\alpha} + \frac{1}{Bi}\right) \tag{25}$$

In dimensional terms, it is

$$t_1 = \frac{\rho_p q_m R^2}{3C_{bo}D_e}\left[\frac{1}{2} + \frac{3(1-\epsilon)VD_e}{FR^2} + \frac{D_e}{k_m R}\right] \tag{26}$$

We can draw a few conclusions here. When $3(1 - \epsilon)VD_e/FR^2$ and D_e/k_mR are less than unity (i.e., large flow rate, low effective diffusivity, and large mass transfer coefficient), the dimensional time required for the adsorption front to reach the particle center of the first cell is

$$t_1 = \frac{\rho_p q_m R^2}{6C_{bo}D_e} \tag{27}$$

i.e., the time required for the adsorption front to reach the particle center of the first mixing cell is proportional to the adsorption capacity q_m to the square of the particle size (L), inversely proportional to inlet concentration and inversely proportional to the effective diffusivity. On the other hand, when

$$\frac{3(1-\epsilon)VD_e}{FR^2} \gg \frac{1}{2}, \frac{D_e}{k_m L} \tag{28}$$

which is likely the case in all adsorption experiments, t_1 is given by

$$t_1 = \frac{(1-\epsilon)V\rho_p q_m}{C_{bo}F} \tag{29}$$

i.e., t_1 is proportional to (a) the maximum adsorption capacity (q_m) and (b) the particle size (R) and is inversely proportional to (a) the inlet concentration (C_{bo}) and (b) the flow rate (F).

Because $T_n < T_{n+1}$, Eq. 20 can be written as

$$1 + 2\left(\frac{\beta}{\alpha}\right) + \frac{2}{Bi} = 6\int_0^{T_n} A_{bo}^n\, d\tilde{t} + 6\int_{T_n}^{T_{n+1}} A_{bo}^n d\tilde{t} \tag{30}$$

Replacing the superscript $(n + 1)$ of Eq. 14 by n by integrating the resulting equation with respect to time $\tilde{t}$ from 0 to T_n yields

$$6\int_0^{T_n} A_b^n d\tilde{t} = 1 + \frac{2}{Bi} \tag{31}$$

Thus, combining Eqs. 30 and 31 yields

$$\frac{1}{3}\left(\frac{\beta}{\alpha}\right) = \int_{T_n}^{T_{n+1}} A_b^n d\tilde{t} \tag{32}$$

Also, when $T_n < \tilde{t} < T_{n+1}$, $A_b^n = 1$ because all the cells up to the nth cell have already been completely saturated with adsorbed solute. So

$$T_{n+1} - T_n = \frac{1}{3}\left(\frac{\beta}{\alpha}\right) \tag{33}$$

for $n = 1,2, \ldots$. T_1 is given in Eq. 25.

Thus the total time required to saturate the fixed-bed adsorber completely is (by summing up Eq. 33)

$$T_N = \frac{1}{3}\left[\frac{1}{2} + \frac{1}{Bi} + N\left(\frac{\beta}{\alpha}\right)\right] \tag{34}$$

In dimensional terms, it is

$$t_N = \frac{\rho_p q_m R^2}{3C_{bo}D_e}\left[\frac{1}{2} + \frac{D_e}{k_m R} + \frac{3(1-\epsilon)V_T D_e}{FR^2}\right] \tag{35}$$

when V_T is the total fixed-bed adsorber volume. Thus, when

$$\frac{3(1-\epsilon)V_T D_e}{FR^2} \gg \frac{1}{2} \text{ and } \frac{D_e}{k_m R} \tag{36}$$

which is likely the case in most industrial fixed-bed adsorbers, the time required to saturate the fixed-bed adsorber completely is

$$t_N = \frac{(1-\epsilon)V_T \rho_p q_m}{C_{bo}F} \tag{37}$$

It is noted that this time t_N is independent of N (i.e., independent of the axial dispersion effect) and is independent of the effective diffusivity. Thus t_N is proportional to:

- Size of the reactor, V_T.
- The maximum adsorption capacity, q_m.

and is inversely proportional to:

- The inlet concentration, C_{bo}.
- The flow rate, F.

The fact that t_N is independent of N implies that whether the adsorber behaves as a well-mixed adsorber or as a plug-flow adsorber the time t_N is always the same for both cases. This interesting fact has been pointed out in a recent work by Cho et al. (1983) in the context of pore-mouth poisoning.

Solute Profile Along the Fixed-Bed Adsorber

When none of the cells is completely saturated, i.e.

$$0 < \tilde{t} < T_1$$

For this case

$$[1 - (X^1)^2] + \frac{2}{3}\left(\frac{\beta}{\alpha} + \frac{1}{Bi} - 1\right)[1 - (X^1)^3] = 2\tilde{t} \tag{38a}$$

$$A_b^1 = G_1 = \frac{1}{\left[1 + \dfrac{(\beta/\alpha)}{(1/X^1 - 1 + 1/Bi)}\right]} \tag{38b}$$

and for $n = 1,2,3, \ldots, N - 1$

$$h(X^{n+1}) = f(X^n) \tag{39a}$$

$$A_b^{n+1} = \prod_{j=1}^{n+1} G^j \tag{39b}$$

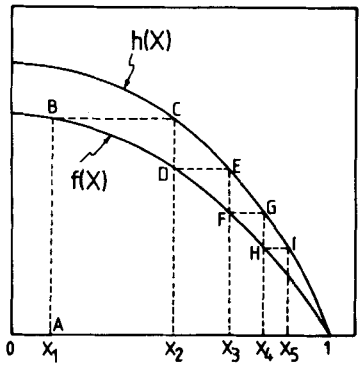

Figure 1. Graphical determination of adsorption front when none of the cells is completely saturated.

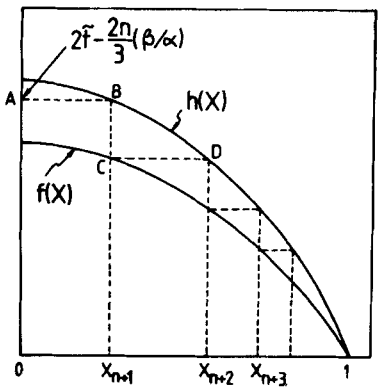

Figure 2. Graphical determination of adsorption front when n cells are completely saturated.

where G^j is given in Eq. 17, and

$$h(X) = (1 - X^2) + \frac{2}{3}\left(\frac{\beta}{\alpha} + \frac{1}{Bi} - 1\right)(1 - X^3) \tag{40}$$

$$f(X) = (1 - X^2) + \frac{2}{3}\left(\frac{1}{Bi} - 1\right)(1 - X^3) \tag{41}$$

Figure 1 shows plots of $h(X)$ and $f(X)$ vs. X. Equations 38a and 39a define the operating lines of the adsorption process through cell-by-cell stagewise graphical construction. The graphical construction is made as follows:

1. For a given time t, the adsorption front X_1 is given explicitly in Eq. 38a. This yields point A in Figure 1.
2. Draw a vertical line; this line intersects the line $f(X)$ at point B, for which the ordinate is $f(X_1)$.
3. Draw a parallel line from B; this line intersects the line $h(X)$ at point C. This gives X_2 and $h(X_2) = f(X_1)$ (Eq. 39a).
4. The same procedure can be carried out to obtain $X_3, X_4, \ldots$.

The solute concentration of each cell can be calculated from Eq. 39b.

Solute Profile Along the Fixed-Bed Adsorber

When some of the cells are already completely saturated, the above graphical procedure has to be modified (same procedure was originally carried out by Cho et al., 1983). To illustrate this modified procedure, we assume that all the cells up to the nth cell are completely saturated with adsorbate. Then for

$$t_n < \tilde{t} < T_{n+1} \tag{42a}$$

$$X_j = 0, A_b^j = 1, \text{ for } j = 1,2, \ldots, n \tag{42b}$$

Thus, for the $(n + 1)$th cell, Eq. 18 can be rewritten as

$$h(X^{n+1}) = 2\int_0^{T_n} A_b^n d\tilde{t} + 2\int_{T_n}^{\tilde{t}} A_b^n d\tilde{t} \tag{43}$$

The first term in the right-hand side of Eq. 43 is $f(0)$, as resulted from Eqs. 14 and 16. And since $A_b^n = 1$, Eq. 43 becomes

$$h(X^{n+1}) = f(0) + 2(\tilde{t} - T_n) \tag{44}$$

Combining Eqs. 25 and 33 gives

$$T_n = \frac{1}{2}f(0) + \frac{n}{3}\left(\frac{\beta}{\alpha}\right) \tag{45}$$

Thus Eq. 44 becomes

$$h(X^{n+1}) = 2\tilde{t} - \frac{2n}{3}\left(\frac{\beta}{\alpha}\right) \tag{46}$$

for $T_n < \tilde{t} < T_{n+1}$

For the jth cell $(j \geq n + 2)$, we still have

$$h(X^j) = f(X^{j-1}) \tag{47}$$

Equations 46 and 47 define the operating lines of the adsorption process when all the cells up to the nth cell are already completely saturated with adsorbed solute. The modified graphical procedure is now as follows (Figure 2):

1. Equation 46 determines point A.
2. Draw a parallel line from A that cuts the h curve at B, of which the coordinates are X^{n+1} and $h(X^{n+1})$.
3. Draw a vertical line from B that cuts the f curve at C and then draw a parallel line from C that cuts the h curve at D, of which the coordinates are X^{n+2} and $h(X^{n+2})$.
4. The same procedure can be carried out to determine X^{n+3}, X^{n+4}, and so on.

Performance of Fixed-Bed Adsorber

The performance of a fixed-bed adsorber is often judged by the breakthrough curve, i.e., the solute concentration of the Nth cell vs. time. Generally, one would like to determine time at which the solute concentration of the Nth cell is a fraction of the inlet concentration, fC_{bo} $(f < 1)$. This time can be determined graphically and iterately as follows (see Figure 3):

1. Choose the adsorption front X^N for the final mixing cell.
2. Draw the operating lines (vertical and parallel lines) in a backward fashion $ABCDEFGH$. The ordinate of point H is

$$h(X^{N-j}) = 2\tilde{t} - \frac{2}{3}(N - j - 1)\left(\frac{\beta}{\alpha}\right) \tag{48}$$

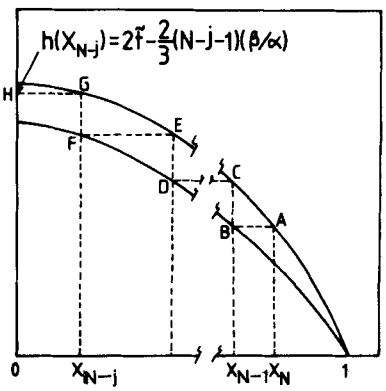

Figure 3. Graphical determination of the breakthrough curve.

from which $\tilde{t}$ can be calculated.

3. We then have

$$X^i = 0 \ (i = 1,2, \ldots, N-j-1) \tag{49a}$$

$$A_b^i = 1 \ (i = 1,2, \ldots, N-j-1) \tag{49b}$$

4. And finally

$$A_b^N = \prod_{i=N-j}^{N} G^i \tag{50}$$

where G^i is given in Eq. 17.

5. If A_b^N in Eq. 50 is not equal to f ($f < 1$), the adsorption front X^N has to be rechosen and the procedure is restarted from step 1 until the exit concentration is equal to fC_{bo}.

DISCUSSION

The theoretical analysis of a fixed-bed adsorber for systems having a rectangular adsorption isotherm (the flat part of a Langmuir isotherm or an irreversible isotherm) has been thoroughly carried out using a discrete cell model. The analysis has resulted in a simple graphical procedure to determine the solute concentration and the adsorption front (X) along the fixed-bed adsorber at any instant of time. Importantly, the analysis also provides a simple procedure to determine the breakthrough curve of the system.

The rectangular adsorption isotherm is commonly observed in many experiments of adsorption of organic solutes in aqueous phase into activated carbon. Therefore our theory is particularly applicable to these liquid phase systems. However, any gas phase systems having rectangular adsorption isotherm can also be analyzed by our theory.

Before discussing in detail the graphical procedure, we would like to mention the time scale used in the analysis. The nondimensional time scale used is (Eq. 11)

$$\tilde{t} = \psi\tau = \frac{\epsilon_p C_{bo}}{\rho_p q_m} \cdot \frac{D_e t}{\epsilon_p R^2} \tag{51}$$

It is seen in Eq. 51 that this nondimensional time $\tilde{t}$ has been scaled with respect to the pore diffusion time and been corrected by the adsorptive capacity term ($C_{bo}/\rho_p q_m$). This is important because the breakthrough curve occurs when the magnitude of t is about at the order of unity (Eq. 34); therefore, a system having a large adsorption capacity (high q_m) or having a low feed concentration will have long lifetime.

In a previous section we showed theoretically that the time (nondimensional) it takes for the adsorber to be fully saturated with adsorbate is

$$T_N = \frac{1}{3}\left[\left(\frac{1}{2}\right) + \frac{1}{Bi} + \frac{N\beta}{\alpha}\right] \tag{52}$$

where N is the number of cells, and β and α are defined in Eq. 8c. This nondimensional completion time is function of Bi and $N\beta/\alpha$. The latter, when written in terms of dimensional parameters, is

$$\frac{N\beta}{\alpha} = \frac{3(1-\epsilon)D_e L}{\bar{u}R^2} \tag{53}$$

where ϵ is the bed voidage and $\bar{u}$ is the superficial velocity. Therefore it is clear that the completion time is independent of the number of cells, i.e., it is independent of the degree of axial mixing. Although this completion time by itself is not an indicator of the performance of the adsorber, it is still useful to investigate this time one step further. Equation 52, when written in terms of dimensional parameters, is

$$t_N = \frac{\rho_p q_m}{3C_{bo}}\left[\frac{R^2}{2D_e} + \frac{R}{k_m} + \frac{3(1-\epsilon)L}{\bar{u}}\right] \tag{54}$$

It is now seen that three dynamic time scales—pore diffusion time, external mass transfer time, and fluid residence time—all contribute to the completion time in an additive fashion, i.e.

Completion time = (Adsorptive capacity)(Pore diffusion time + external mass transfer time + residence time)

The external mass transfer time is usually the smallest among those three time scales.

If the pore diffusion time is greater than the fluid residence time (i.e., for systems having very high fluid velocity, a very rare case in adsorption studies), the completion time is

$$t_N \cong \frac{1}{6} \cdot \frac{\rho_p q_m}{C_{bo}} \cdot \frac{R^2}{D_e} \tag{55}$$

Surprisingly, this completion time is independent of fluid velocity. However, when we consider the physical aspects of the system, this will come as no surprise at all. When the fluid residence time is much less than the pore diffusion time, the interparticle concentrations along the fixed-bed adsorber are equal to the inlet concentration before the adsorbate species diffuse into the pores of the adsorbents. Therefore the completion time is dominated solely by the pore diffusion time. This case, however, must be avoided when designing a fixed-bed adsorber. For example, for a liquid phase adsorber to be designed with $R = 0.05$ cm, $D_e = 5 \times 10^{-6}$ cm^2/s, and $\epsilon = 0.5$, a designer must choose a liquid residence time of not less than

$$\frac{R^2}{6(1-\epsilon)D_e} = \frac{(0.05)^2}{6(1-0.5)(5\times 10^{-6})} = 167 \text{ s}$$

When the fluid residence time is greater than the pore diffusion time, which is the case in *all* adsorption systems, the completion time is

$$t_N \cong \frac{(1-\epsilon)\rho_p q_m}{C_{bo}} \cdot \frac{L}{\bar{u}} \tag{56}$$

Thus the completion time is proportional to the fluid residence time and to the adsorptive capacity of the adsorbent. Therefore, to improve the lifetime of an adsorber, one could increase the fluid residence time. This, however, reduces the throughput of the system. One can also improve its lifetime by choosing adsorbents having high adsorptive capacity (i.e., high q_m). Activated carbon having high internal surface area and high affinity to many organic solutes in aqueous phase is therefore a popular adsorbent for use by many researchers in many fields. As we have pointed out, this case is the one observed in all adsorption systems; therefore the first criterion in designing a fixed-bed adsorber is

$$N(\beta/\alpha) > 1 \tag{57a}$$

or

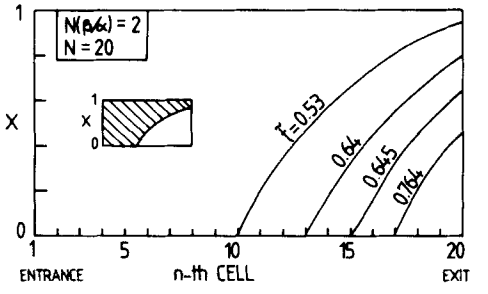

Figure 4. Typical adsorption front profile along the adsorber for ($N\beta/\alpha$) = 2.

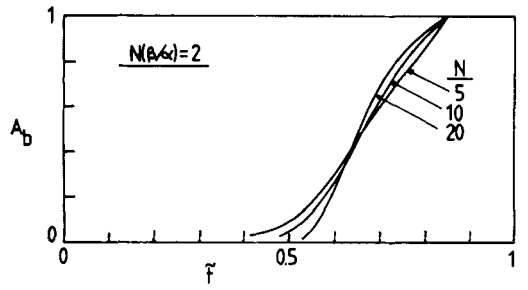

Figure 5. Effect of N on the breakthrough curve for $(N\beta/\alpha) = 2$.

$$\frac{L}{\bar{u}} > \frac{R^2}{6(1-\epsilon)D_e} \tag{57b}$$

The constraint criterion of Eq. 57a will be used in subsequent simulations.

The procedure of calculating the solute profile and the adsorption front along a fixed-bed adsorber was described in detail in previous sections for the case when none of the cells is completely saturated and for when some of the cells are fully saturated. Figure 4 shows a typical adsorption front profile along the adsorber when $N\beta/\alpha = 2$ and the number of cells is 20. The shaded area corresponds to the portion of the adsorbent saturated with the adsorbate. For example, when $\tilde{t} = 0.531$, all the cells up to the tenth cell are completely saturated with the adsorbate and the remaining cells are only partially saturated. In the fourteenth cell, for instance, 81% of $((1 - X^3) = (1 - 0.57^3))$ of the adsorbent volume is saturated with the adsorbate. Figure 4 is useful in showing how the adsorption front profile varies with time.

The information that any practical engineer would like to know is the prediction of the breakthrough curve. The procedure of determining it (the algorithm, Eqs. 48–50) has been described in a previous section. Figure 5 shows a plot of the exit concentration vs. time (i.e., the breakthrough curve) for $(N\beta/\alpha) = 2$ and $N = 5$, 10, and 20. Various values of N correspond to various degrees of axial mixing. The smaller the value of N, the higher the degree of axial mixing. As observed by many investigators in their analyses of a fixed-bed adsorber having a linear adsorption isotherm, we also observe here for a fixed-bed adsorber having a rectangular adsorption isotherm that the breakthrough curve is sharper when the axial mixing is reduced. However, such dependence of the breakthrough curve on the axial mixing is not significant. This axial mixing effect is not as strong as other physicochemical effects.

For a given degree of axial mixing, the effect of velocity is shown in Figure 6 for various values of $(N\beta/\alpha)$. It is seen in the figure that the shape of the breakthrough curve is almost fixed irrespective of the values of $(N\beta/\alpha)$. The nondimensional time to saturate the adsorber, i.e., the time at which the exit concentration is unity, is given in Eq. 52. Figure 6 is very useful to design engineers to

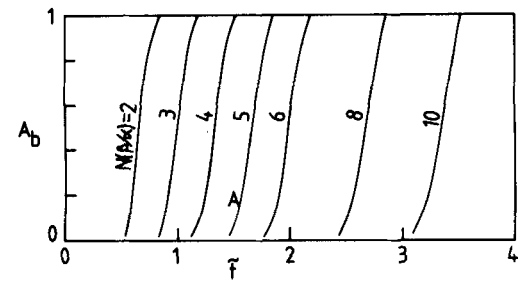

Figure 6. Effect of $(N\beta/\alpha)$ on the breakthrough curve with $N = 20$.

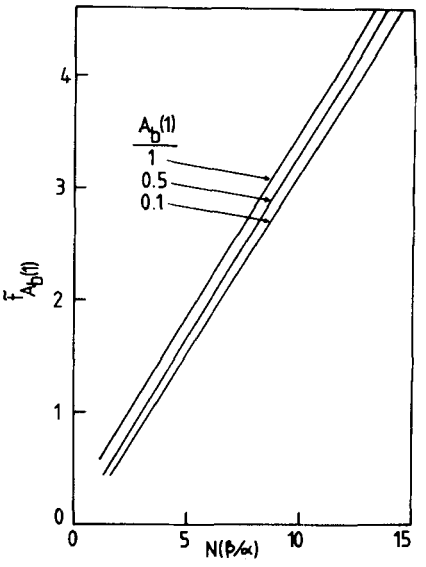

Figure 7. Plot of $\tilde{t}_{A_b}$ vs. $(N\beta/\alpha)$ with A_b as parameter.

predict the performance of a fixed-bed adsorber. For example, the following information is given to a design engineer:

$$R = 0.05 \text{ cm}$$
$$D_e = 5 \times 10^{-6} \text{ cm}^2/\text{s}$$
$$L = 10 \text{ cm}$$
$$\bar{u} = 0.006 \text{ cm/s}$$
$$\epsilon = 0.5$$
$$q_m = 0.2 \text{ g/g}$$
$$\rho_p = 1 \text{ g/cm}^3$$
$$C_{bo} = 1 \times 10^{-4} \text{ g/cm}^3$$

The design question is what is the lifetime of the adsorber if not more than 20% of the inlet concentration is allowed to pass through the adsorber.

First, he calculates

$$N\beta/\alpha = \frac{3(1-0.5)(5\times10^{-6})(10)}{(0.15)(0.05)^2} = 5$$

$$Re = \frac{\bar{u}d_p\rho}{\mu} = \frac{(0.006)(0.1)(1)}{0.0095} = 0.063$$

The Reynolds number is used to calculate the Peclet number . Using the following correlation for liquid phase axial dispersion in fixed bed (Wen and Fan, 19754)

$$\epsilon Pe = 0.2 + 0.011Re^{0.48}$$

the Peclet number is calculated as 0.406. Therefore, the number of cells required by the discrete model is

$$N = \frac{Pe}{2}\left(\frac{L}{d_p}\right) = \frac{0.406}{2}\left(\frac{10}{0.1}\right) \cong 20$$

Thus, having $(N\beta/\alpha) = 5$ and $N = 20$, the curve marked A in Figure 6 represents the breakthrough curve for the given information. The nondimensional time at which the exit concentration is 0.2 is 1.58, and therefore the real time

$$t = \frac{1.58R^2\rho_p q_m}{C_{bo}D_e} = \frac{1.58(0.05)^2(1)(0.2)}{(1\times10^{-4})(5\times10^{-6})}$$

$$t = 1{,}580{,}000 \text{ s} \cong 440 \text{ h}$$

Hence the lifetime of the fixed-bed adsorber is 440 h. This long lifetime is attributed to the fact that low velocity is used in the

TABLE 2. COMPARISON OF $\tilde{t}$ BETWEEN OUR SOLUTION (EQ. 58) AND HALL ET AL. SOLUTION (EQ. 59) FOR BI = 20 AND $N\beta/\alpha = 5$

X	0.01	0.1	0.2	0.3	0.4	0.5	0.6	0.7	0.8	0.9	0.99
$\tilde{t}$ (our solution)	1.50	1.53	1.57	1.60	1.64	1.67	1.71	1.74	1.78	1.81	1.85
$\tilde{t}$ (Hall et al.)	1.53	1.57	1.60	1.62	1.64	1.66	1.69	1.71	1.73	1.77	1.83

calculation. It is interesting to note that the fluid residence time is ($L/\bar{u}$ = 0.463 h) and hence the adsorption process retards the emergence of the adsorbate from the adsorber by a factor of 950 (=440/0.463).

We note the constant pattern of the breakthrough curve in Figure 6. Thus if we plot the time at which the exit concentration is $A_b(1)$ vs. ($N\beta/\alpha$) for three values of $A_b(1)$ (0.2, 0.5, and 1), the result is shown in Figure 7. These three curves are almost parallel to each other. This substantiates the constant pattern of the breakthrough curve, as observed in Figure 6. The straight line corresponding to $A_b(1) = 1$ is, in fact, the graphical version of Eq. 52. Utilizing the fact that the three lines in Figure 7 are parallel to each other, we are able to obtain the following analytical expression for $\tilde{t}_{A_b}(1)$, which is the time (nondimensional) at which the exit concentration is equal to $A_b(1)$:

$$\tilde{t}_{A_b(1)} = \frac{1}{3}\left[\left(\frac{1}{2} + \frac{1}{Bi}\right)(-0.942 + 1.942A_b(1)) + \left(\frac{N\beta}{\alpha}\right)\right] \quad (58)$$

where ($N\beta/\alpha$) is given in Eq. 53 and the nondimensional time has been scaled as in Eq. 51. It is interesting to compare our solution (58) with the solution obtained by Hall et al. (1966). When written in terms of our variables and parameters, their solution is

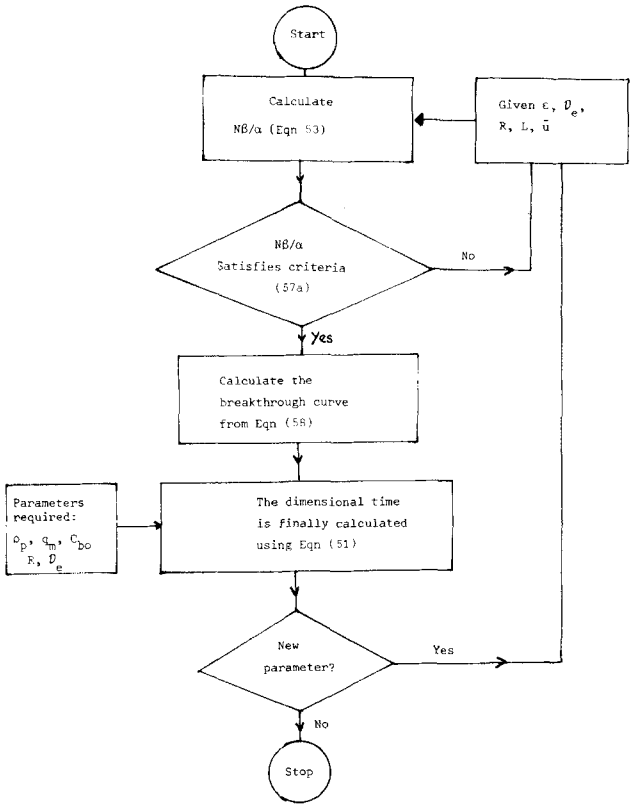

Figure 8. Design algorithm.

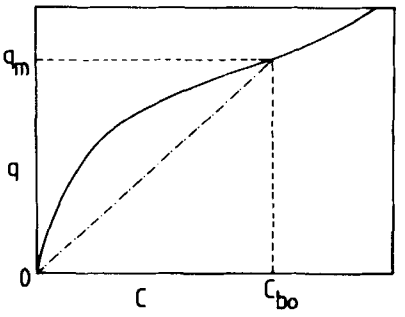

Figure 9. An arbitrary nonlinear isotherm.

$$\tilde{t}_{A_b(1)} = \frac{1}{15}[5(N\beta/\alpha) + \Phi(A_b(1)) + \frac{5}{Bi}(\ln X + 1)] \quad (59)$$

where Φ is defined in Appendix II of their paper. Table 2 compares the effluent times vs. $A_b(1)$ for Bi = 20 and ($N\beta/\alpha$) = 5, and it is not surprising to see how close these two solutions are. However, our solution is explicit and is ready to use on a desk calculator.

Thus the design procedure for a fixed-bed adsorber for systems having rectangular adsorption isotherm is very simple as described in the algorithm of Figure 8.

The design algorithm described above is simple to apply because all required formulas are explicit and simple. This algorithm will provide design engineers with a quick method to design a fixed bed having a rectangular adsorption isotherm. For *any* arbitrary nonlinear isotherms (Figure 9), this algorithm also provides a convenient method to determine an upper bound of the lifetime of the fixed-bed adsorber. The parameter q_m required in our algorithm is chosen as the adsorbed concentration in equilibrium with the inlet adsorbate concentration (see Figure 9). Solutions of a linear isotherm (see dot-dash line in Figure 9) would provide a conservative lifetime of the fixed-bed adsorber. Therefore this solution, together with the solution obtained in this paper, would provide a lower bound and an upper bound of the real lifetime of the fixed-bed adsorber having a nonlinear adsorption isotherm.

NOTATION

A = nondimensional pore fluid concentration
A_b = nondimensional bulk concentration
A_s = nondimensional adsorbed concentration
Bi = Biot number for mass transfer
C = pore fluid concentration
C_b = bulk concentration
d_p = particle diameter
D_e = pore effective diffusivity
E = axial dispersion coefficient
$f(X)$ = defined in Eq. 41
F = volumetric flow rate
G = defined in Eq.17
$h(X)$ = defined in Eq. 40

k = adsorption rate constant
k_m = mass transfer coefficient
N = number of cells
Pe = Peclet number
q = adsorbed concentration
q_m = maximum adsorbed concentration
r = radial coordinate
R = particle radius
t = time
$\tilde{t}$ = nondimensional time, defined in Eq. 11
T_n = time to saturate the nth cell
T_N = time to saturate the whole adsorber, Eq. 34
$\bar{u}$ = superficial velocity
V = volume of one cell
V_T = adsorber volume
x = nondimensional radial coordinate
X = adsorption front

Greek Letters

α = defined in Eq. 8c
β = defined in Eq. 8c
ϵ = bed voidage
ϵ_p = particle voidage
μ = defined in Eq. 13
ϕ = defined in Eq. 8b
π_p = particle density
ρ = nondimensional time
ψ = defined in Eq. 8c

Superscript

n = nth cell

LITERATURE CITED

Andrieu, J., and J. M. Smith, "Rate Parameters for Adsorption of CO_2 in Beds of Carbon Particles," *AIChE J.*, **26**, 944 (1980.

Brauch, V., and E. U. Schlünder, "The Scale-up of Activated Carbon Columns for Water Purification, Based on Results from Batch Tests. II," *Chem. Eng. Sci.*, **30**, 539 (1975).

Carleton, F. B., L. S. Kershenbaum, and W. A. Wakeham, "Adsorption in Non-Isobaric Fixed Beds," *Chem. Eng. Sci.*, **33**, 1239 (1978).

Cho, B. K., L. L. Hegedus, and R. Aris, "Discrete Cell Model of Pore-Mouth Poisoning of Fixed-Bed Reactors," *AIChE J.*, **29**, 289 (1983).

Cole, J. D., *Perturbation Methods in Applied Mathematics*, Blaisdell, Waltham, MA (1968).

Colwell, C. J., and J. S. Dranoff, "Nonlinear Equilibrium and Axial Mixing Effects in Intraparticle Diffusion—Controlled Sorption by Ion-Exchange Resin Beds," *Ind. Eng. Chem. Fund.*, **8**, 193 (1969).

Cooper, R. S., and D. A. Liberman, "Fixed Bed Adsorption Kinetics with Pore Diffusion Control," *Ind. Eng. Chem. Fund.*, **9**, 620 (1970).

Crittenden, J. C., et al., "Mathematical Model of Sequential Loading in Fixed Bed Adsorbers," *J. Water Pollution Control Fed.*, **52**, 2780 (1980).

Deans, H. A., and L. Lapidus, "A Computational Model for Predicting and Correlating the Behavior of Fixed-Bed Reactors. I. Derivation of Model for Nonreactive Systems," *AIChE. J.*, **6**, 656 (1960).

Do, D. D., "On the Validity of the Shrinking Core Model in Noncatalytic Gas Solid Reaction," *Chem. Eng. Sci.*, **37**, 1477 (1982).

Do, D. D., and R. H. Weiland, "Deactivation of Single Catalyst Particles at Large Thiele Modulus. Travelling Wave Solutions," *Ind. Eng. Chem. Fund.*, **20**, 48 (1981).

Galan, M. A., M. Suzuki, and J. M. Smith, "Effect of Adsorption Characteristics on Pulse Retention Times," *Ind. Eng. Chem. Fund.*, **14**, 273 (1975).

Hall, K. R., et al., "Pore and Solid Diffusion Kinetics in Fixed Bed Adsorption Under Constant Pattern Conditions," *Ind. Eng. Chem. Fund.*, **5**, 212 (1966).

Hashimoto, N., and J. M. Smith, "Macropore Diffusion in Molecular Sieve Pellets by Chromatography," *Ind. Eng. Chem. Fund.*, **12**, 353 (1973).

Johansson, R., and I. Neretnieks, "Adsorption on Activated Carbon in Countercurrent Flow—An Experimental Study," *Chem. Eng. Sci.*, **35**, 979 (1980).

Kumar, R., R. C. Duncan, and D. M. Ruthven, "A Chromatographic Study of Diffusion of Single Components and Binary Mixtures of Gases in 3A and 4A reolites," *Can. J. Chem. Eng.*, **60**, 493 (1982).

Lee, D. I., S. Kaguei, and N. Wakao, "Relation Between Adsorption Equilibrium Constant, Fluid Dispersion Coefficient and Intraparticle Effective Diffusivity in Time-Domain Analysis of Adsorption Chromatography Curves," *J. Chem. Eng. Jap.*, **14**, 161 (1981).

Lee, D. I., et al., "Short Beds for Chromatographic Measurement of Adsorption Equilibrium Constants," *J. Chem. Eng. Jap.*, **15**, 232 (1982).

Masamune, S., and J. M. Smith, "Adsorption Rate Studies—Significance of Pore Diffusion," *AIChE J.*, **10**, 246 (1964).

Miura, K., et al., "A Method for Calculating Breakthrough Curves of Bicomponent Fixed Bed Adsorption Under Constant Pattern and Linear Driving Force," *J. Chem. Eng. Jap.*, **12**, 281 (1979).

Miura, K., A. Nakanishi, and K. Hashimoto, "Treatment of the Poisonous Gas Remaining After Fumigation by Use of an Activated Carbon Adsorber," *Ind. Eng. Chem. Proc. Des. Dev.*, **22**, 469 (1983).

Neretnieks, I., "Adsorption of Components Having a Saturation Isotherm," *Chem. Eng. Technol.* **46**, 781 (1974).

Ozil, P., and L. Bonnetain, "Dynamical Adsorption in Fixed Bed," *Chem. Eng. Sci.*, **32**, 303 (1977).

Rimpel, A. E., et al., "Kinetics of Physical Adsorption of Propane from Helium on Fixed Beds of Activated Alumina," *AIChE J.*, **14**, 19 (1968); *Chem. Eng. Progr. Symp. Ser. No. 74*, **63**, 53 (1967).

Santacesaria, E., et al., "Separation of Xylenes on Y Zeolites. 2. Breakthrough Curves and Their Interpretation," *Ind. Eng. Chem. Proc. Des. Dev.*, **21**, 446 (1982).

Schneider, P., and J. M. Smith, "Adsorption Rate Constants from Chromatography," *AIChE J.*, **14**, 762 (1968a).

——, "Chromatographic Study of Surface Diffusion," *AIChE J.*, **14**, 886 (1968b).

Seirafi, H. A., and J. M. Smith, "Mass Transfer and Adsorption in Liquid Full and Trickle Beds," *AIChE J.*, **26**, 711 (1980).

Shah, D. B., and D. M. Ruthven, "Measurement of Zeolite Diffusivities and Equilibrium Isotherms by Chromatography," *AIChE J.*, **23**, 804 (1977).

Suzuki, M., and K. Kawazoe, "Batch Measurement of Adsorption Rate in an Agitated Tank," *J. Chem. Eng. Jap.*, **7**, 346 (1974).

Spahn, H., and E. U. Schlünder, "The Scale-up of Activated Carbon Columns for Water Purification, Based on Results from Batch Tests. I," *Chem. Eng. Sci.*, **30**, 529 (1975).

Van Vliet, B. M., W. J. Weber, and H. Hozumi, "Modelling and Prediction of Specific Compound Adsorption by Activated Carbon and Synthetic Adsorbents," *Water Res.*, **14**, 1719 (1980).

Weber, W. J. Jr., and K. T. Liu, "Determination of Mass Transport Parameters for Fixed Bed Adsorbers," *Chem. Eng. Commun.*, **6**, 49 (1980).

Wen, C. Y., and L. T. Fan, *Models for Flow Systems and Chemical Reactors*, Marcel Dekker, New York (1975).

Manuscript received Feb. 15, 1984; revision received June 22, and accepted Sept. 10, 1984.